

Unparticle self-interactions and their collider implications

Jonathan L. Feng, Arvind Rajaraman, and Huitzu Tu

Department of Physics and Astronomy, University of California, Irvine, California 92697, USA

(Received 23 January 2008; published 17 April 2008)

In unparticle physics, operators of the conformal sector have self-interactions, and these are unsuppressed for strong coupling. The 3-point interactions are completely determined by conformal symmetry, up to a constant. We do not know of any theoretical upper bounds on this constant. Imposing current experimental constraints, we find that these interactions mediate spectacular collider signals, such as $pp \rightarrow \mathcal{U} \rightarrow \mathcal{U}\mathcal{U} \rightarrow \gamma\gamma\gamma\gamma, \gamma\gamma ZZ, ZZZZ, \gamma\gamma l^+ l^-, ZZ l^+ l^-,$ and $4l$, with cross sections of picobarns or larger at the large hadron collider. Self-interactions may therefore provide the leading discovery prospects for unparticle physics.

DOI: 10.1103/PhysRevD.77.075007

PACS numbers: 12.60.-i, 11.25.Hf, 13.85.-t, 14.80.-j

I. INTRODUCTION

In unparticle physics, the standard model (SM) is extended by couplings to a conformal sector through interactions of the form OO_{SM} , where O is an operator of the conformal sector, and O_{SM} is a standard model operator [1]. The conformal sector may be weakly coupled [2] or strongly coupled [3], but in all cases, the conformality of the new sector leads to effects that cannot be explained in terms of standard particle states.

To date, all unparticle studies are based on two key elements: the unparticle phase space, and the unparticle propagator. Conformal invariance fixes unparticle phase space [1], which enters processes with unparticles in the final state, such as $f\bar{f} \rightarrow f\mathcal{U}$. Similarly, conformal invariance dictates the form of the unparticle propagator [4,5], which determines virtual unparticle contributions to processes such as $f\bar{f} \rightarrow \mathcal{U} \rightarrow f\bar{f}$. The forms of the unparticle phase space and propagator imply that unparticles do not behave as standard particles, but are more aptly interpreted as fractional numbers of massless particles [1] or as collections of particles with a particular distribution of masses [6]. These results are valid if the couplings of unparticles to the standard model are all nonrenormalizable. If unparticle couplings include the super-renormalizable operator Oh^2 , where h is the standard model Higgs boson, electroweak symmetry breaking breaks conformal invariance [7,8]. This modifies the unparticle propagator and implies that unparticle physics may be probed only in a narrow conformal window, typically at energies between 10 GeV and 1 TeV [7,9]. Such energies are best probed at high energy colliders, and many studies have investigated the collider implications of unparticles [1,4,5,9–12]. Models with conformal breaking may also share characteristics with hidden valley models [13,14].

Here we study a qualitatively new effect: unparticle self-interactions. Such 3- and higher-point interactions are always present in conformal theories, and mediate processes such as $gg \rightarrow \mathcal{U} \rightarrow \mathcal{U} \cdots \mathcal{U}$, with two or more unparticles in the final state. In the most interesting cases with strongly-coupled conformal sectors, the creation of addi-

tional high p_T unparticles in the final state does not suppress the rate. Multi- \mathcal{U} production therefore differs from all known examples, such as $gg \rightarrow g \rightarrow g \cdots g$ and $gg \rightarrow \gamma \cdots \gamma$, where the rate is reduced with the addition of every high p_T particle.

In this paper, we focus on 3-point self-interactions. These are the natural starting point for several reasons. First, unlike 4- and higher-point self-interactions, 3-point interactions are completely constrained by conformal invariance, up to a constant. Second, 3-point interactions are the leading order at which induced signals may be nearly background free. For example, although the \mathcal{U} propagator induces signals like $pp \rightarrow \mathcal{U} \rightarrow \gamma\gamma$, 3-point \mathcal{U} self-interactions mediate $pp \rightarrow \mathcal{U} \rightarrow \mathcal{U}\mathcal{U} \rightarrow \gamma\gamma\gamma\gamma, \gamma\gamma ZZ, ZZZZ, \gamma\gamma l^+ l^-, ZZ l^+ l^-, 4l$, and many other spectacular signals through subprocesses such as the one shown in Fig. 1. For this reason, the most promising signals for unparticle discovery at colliders may in fact be those that are induced by 3-point unparticle interactions. (Note that, although the production of three or more unparticles may also be unsuppressed, the requirement that they convert back to standard model particles to be visible does, in fact, imply that these are subdominant.)

In the following sections, we start from the 3-point correlation function in position space and convert it to a

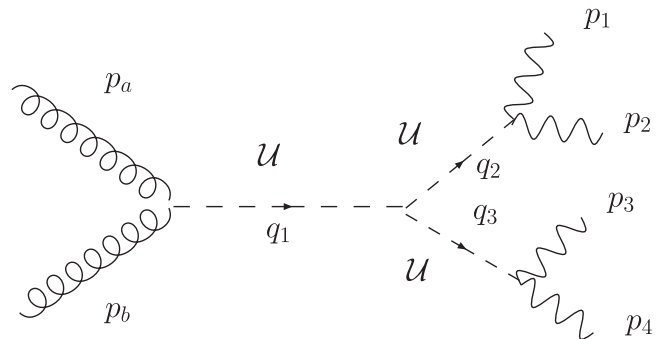


FIG. 1. The process $gg \rightarrow \gamma\gamma\gamma\gamma$ mediated by unparticle self-interactions.

form useful for Feynman diagram calculations. We then calculate collider rates, taking the 4γ signal as our example. Our final result is determined up to the constant entering the 3-point correlation function. As far as we know, there is no theoretical upper bound on this constant—it is bounded only by current experimental constraints. Applying these constraints, we find that the prospects for signals at the large hadron collider (LHC) are truly spectacular—the four-body final states given above may have cross sections of picobarns or larger, leading to obvious signals visible in the first year of the LHC. We also determine the predicted kinematic distributions from unparticles, which are insensitive to overall rates. These distributions provide testable predictions that could be used to distinguish multiunparticle production from other possibilities for new physics.

II. 3-POINT CORRELATION FUNCTION

We begin by assuming that the standard model is coupled to the unparticle sector through a scalar operator O . For a scalar, unitarity requires dimension $d \geq 1$, but there is no upper bound [15,16]. Motivated by prominent supersymmetric examples [3], we consider the range $1 \leq d < 2$. Modifications are required for vector and tensor operators [15–17], but we expect that our primary conclusions apply to these cases as well.

Conformal invariance constrains the 3-point O correlation function to be

$$\langle 0|O(x)O(y)O^\dagger(0)|0\rangle = \frac{C'_d}{|x-y|^d|x|^d|y|^d}, \quad (1)$$

where C'_d is a constant determined by the unparticle self-coupling strength. In momentum space, it is then

$$\begin{aligned} & \langle 0|O(p_1)O(p_2)O^\dagger(p_1+p_2)|0\rangle \\ &= C'_d \int d^4x d^4y \frac{1}{|x-y|^d|x|^d|y|^d} e^{ip_1 \cdot x} e^{ip_2 \cdot y} \\ &= C'_d \int d^4x d^4y d^4z \delta^4[z-(x-y)] \frac{1}{|z|^d|x|^d|y|^d} e^{ip_1 \cdot x} e^{ip_2 \cdot y} \\ &= C'_d \int \frac{d^4q}{(2\pi)^4} \int d^4x d^4y d^4z \frac{e^{iq \cdot [z-(x-y)]} e^{ip_1 \cdot x} e^{ip_2 \cdot y}}{|z|^d|x|^d|y|^d} \\ &= C_d \int \frac{d^4q}{(2\pi)^4} [-q^2 - i\epsilon]^{(d/2)-2} [-(p_1 - q)^2 - i\epsilon]^{(d/2)-2} \\ & \quad \times [-(p_2 + q)^2 - i\epsilon]^{(d/2)-2}, \end{aligned} \quad (2)$$

where the last equality makes use of the unparticle 2-point correlation function [4]. C_d is determined in terms of C'_d ; we choose to express our results in terms of C_d .

The 3-point correlation function is the product of three propagators from 0 to x , x to y , and y to 0. It is therefore not surprising that, in momentum space, it takes the form of a loop integral. We may therefore make use of the standard techniques available for simplifying loop calculations.

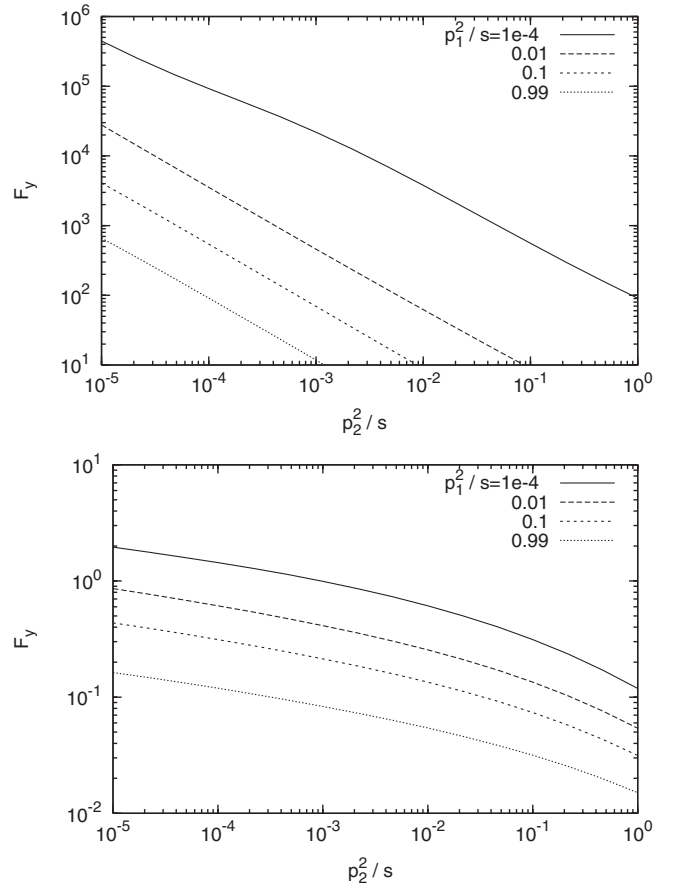


FIG. 2. Feynman parameter integral $F_y(p_1^2/s, p_2^2/s)$, as a function of p_2^2/s for several p_1^2/s values and $d = 1.1$ (top) and 1.9 (bottom).

Using Feynman parameters for Eq. (2), the 3-point correlation function becomes

$$\begin{aligned} & \langle 0|O(p_1)O(p_2)O^\dagger(p_1+p_2)|0\rangle \\ &= -i(-1)^n C_d \left(\frac{1}{s}\right)^{n-2} F_y\left(\frac{p_1^2}{s}, \frac{p_2^2}{s}\right), \end{aligned} \quad (3)$$

where

$$\begin{aligned} F_y\left(\frac{p_1^2}{s}, \frac{p_2^2}{s}\right) &= \frac{1}{16\pi^2} \frac{\Gamma(n-2)}{[\Gamma(\frac{n}{3})]^3} \\ & \quad \times \int_0^1 dx_1 dx_2 dx_3 \delta(x_1 + x_2 + x_3 - 1) \\ & \quad \times \left(\frac{1}{\Delta'}\right)^{n-2} (x_1 x_2 x_3)^{1-(d/2)}, \end{aligned} \quad (4)$$

$n = 6 - \frac{3d}{2}$ and $\Delta' = x_1 x_2 p_1^2/s + x_1 x_3 p_2^2/s + x_2 x_3$, with $s = (p_1 + p_2)^2$. $F_y(p_1^2/s, p_2^2/s)$ is plotted in Fig. 2.

III. BOUNDS ON UNPARTICLE INTERACTIONS

To investigate the phenomenological implications of the 3-point correlation function discussed in Sec. II, we must

introduce unparticle couplings to standard model particles. Here we present the relevant couplings and determine the existing constraints on them and the prospects for probing them at the LHC. The results here are independent of unparticle self-interactions, but are of interest in their own right. In addition, in Sec. IV we will present results for a reference value of Λ_4 , which we choose based on the results we derive here.

A scalar unparticle may couple to two gauge bosons or two fermions through the Lagrangian interaction terms

$$\mathcal{L} = \frac{c_i}{\Lambda_4^d} O F_{\mu\nu}^i F^{i\mu\nu} + \frac{ec_4^f}{\Lambda_4^d} O h \bar{f}_L f_R, \quad (5)$$

leading to the Feynman rules

$$\begin{aligned} O\gamma\gamma, Ogg \text{ vertices: } & i \frac{4c_{\gamma,g}}{\Lambda_4^d} (-p_a \cdot p_b g^{\alpha\beta} + p_a^\beta p_b^\alpha) \\ O\bar{f}f \text{ vertex: } & ie \frac{c_4^f v}{\Lambda_4^d} P_R, \end{aligned} \quad (6)$$

where Λ_4 is some high scale characterizing these non-renormalizable interactions, v is the Higgs vacuum expectation value, e is the proton charge, and c_γ , c_g , and c_4^f are constants.

Following convention, we choose an O normalization by specifying the unparticle propagator [4,5]

$$\text{scalar unparticle propagator: } iB_d \theta(q^0) \theta(q^2) (q^2 - \mu^2)^{d-2}, \quad (7)$$

where

$$B_d \equiv A_d \frac{(e^{-i\pi})^{d-2}}{2 \sin d\pi}, \quad A_d \equiv \frac{16\pi^{5/2} \Gamma(d + \frac{1}{2})}{(2\pi)^{2d} \Gamma(d-1) \Gamma(2d)}. \quad (8)$$

Here the modified propagator suggested in Ref. [7] is used to take into account the breaking of conformal invariance at a scale μ by unparticle couplings to the Higgs boson. A more detailed analysis was performed in Ref. [8] by considering a deconstructed version of the unparticle-Higgs coupling. That approach led to a propagator of the form $[(q^2)^{2-d} - v^2(\mu_U^2)^{2-d}/(q^2 - m_h^2)]^{-1}$, where v and m_h are the Higgs vacuum expectation value and mass, respectively, and μ_U is a scale related to the Higgs-unparticle coupling.

We will be most interested in unparticle couplings to two photons. This coupling, in conjunction with unparticle couplings to gluons and quarks, mediates processes $gg, q\bar{q} \rightarrow \mathcal{U} \rightarrow \gamma\gamma$, which have been studied previously in Ref. [11]. With our coupling conventions, these processes have differential cross sections

$$|\overline{\mathcal{M}}_{g\bar{g} \rightarrow 2\gamma}|^2 = 2 \left| \frac{c_g c_\gamma}{\Lambda_4^{2d}} \right|^2 |B_d|^2 v^2 (\hat{s} - \mu^2)^{2d-4} \hat{s}^3, \quad (9)$$

$$|\overline{\mathcal{M}}_{q\bar{q} \rightarrow 2\gamma}|^2 = \frac{2}{3} \left| \frac{ec_4^f c_\gamma}{\Lambda_4^{2d}} \right|^2 |B_d|^2 v^2 (\hat{s} - \mu^2)^{2d-4} \hat{s}^3, \quad (10)$$

where we have averaged and summed over initial and final state colors and polarizations, but have not yet included the factor 1/2 to account for the two identical photons in the final state.

These processes are bounded by existing data, most stringently by the diphoton invariant mass distribution from the CDF Collaboration at the Tevatron [18], based on an integrated luminosity of 1.2 fb^{-1} at $\sqrt{s} = 1.96 \text{ TeV}$. The events in this distribution have two central photons with $|\eta| < 1.04$ and transverse momenta $p_T^{1,2} \geq 15 \text{ GeV}$. To obtain a lower bound on Λ_4 , we simulate the signal by adopting the following procedure here and in all analyses described below. We set $c_g = c_\gamma = 1$ and $e^2(c_4^f)^2 = 2\pi$, following the convention justified in Ref. [9], use the CTEQ5L parton distribution functions with a factorization scale $\mu_f = \sqrt{\hat{s}}$ [19], and evaluate the cross section with the Monte Carlo program VEGAS [20]. We then impose the identical η and p_T cuts given above, and further require $m_{\gamma\gamma} > M_{\text{th}}$, where $m_{\gamma\gamma}$ is the diphoton invariant mass, and M_{th} is a threshold mass chosen to maximize the sensitivity to the signal. At the Tevatron, unparticle production through $q\bar{q}$ dominates over gg , and the most stringent bounds are typically achieved for $M_{\text{th}} \approx 350 \text{ GeV}$. The 95% CL lower bound on Λ_4 is then derived following Ref. [21]; these results are given in Fig. 3. For comparison, in Fig. 3 we also present bounds on Λ_4 given previously in the literature from $e^+e^- \rightarrow \mathcal{U} \rightarrow \mu^+\mu^-$ from LEP/SLC [9] and the unitarity bound on WW scattering [10].

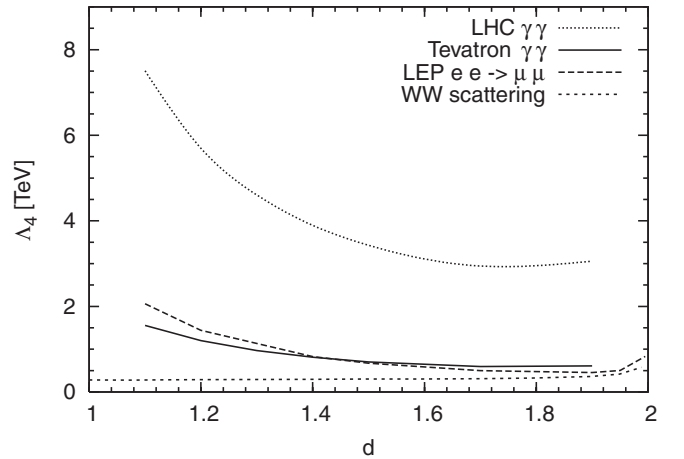


FIG. 3. Bounds on the unparticle scale Λ_4 from $p\bar{p} \rightarrow \mathcal{U} \rightarrow \gamma\gamma$ using existing data from the Tevatron (solid line), and the projected 5σ discovery reach at the LHC for integrated luminosity 100 fb^{-1} (dotted line). For comparison, existing bounds from $e^+e^- \rightarrow \mathcal{U} \rightarrow \mu^+\mu^-$ [9] (long dashed line) and the unitarity bound on WW scattering [10] (short dashed line) are also shown. See text for details.

We have also determined the discovery reach for $pp \rightarrow \mathcal{U} \rightarrow \gamma\gamma$ at the LHC, assuming 100 fb^{-1} of data. We evaluate the prompt diphoton background using PYTHIA 6.4 [22], impose kinematic cuts $|\eta| < 2.5$ and $p_T^{1,2} > 25 \text{ GeV}$, and again optimize by varying the threshold energy M_{th} . We estimate a 5σ discovery reach by requiring $S/\sqrt{B} > 5$ and $S > 5$, where S and B are the number of signal and background events. This discovery reach is also presented in Fig. 3.

These results have omitted important effects. Notably, in determining the LHC reach, we have omitted the background from misidentification of jets and electrons. Nevertheless, we may conclude that present limits from the Tevatron and LEP/SLC are comparable, and imply lower bounds on Λ_4 of $\sim 2 \text{ TeV}$ for $d = 1.1$, dropping to below a TeV for $d = 1.9$. We will adopt the reference value $\Lambda_4 = 1 \text{ TeV}$ below. At the LHC, the sensitivity is much higher, with the $\gamma\gamma$ signal probing Λ_4 in the multi-TeV range. Note that here, and in the rest of this work, we have taken the conformal breaking scale to be $\mu = 0$ in deriving our results. However, we have found that our results are insensitive to this choice, provided $\mu \lesssim M_{\text{th}}$. In general, the modifications have the property that they are small for large q^2 . For example, for $q^2 \gg \mu^2$, the propagator we used [Eq. (7)] is of the form $(q^2)^{d-2}$ with corrections of order μ^2/q^2 . In this limit the propagator obtained from Ref. [8] has corrections of order $(\mu^2/q^2)^{2-d} v^2/(q^2 - m_h^2)$. We will assume henceforth that the breaking of conformal symmetry is small in the kinematic region we work in so that the correction terms can be ignored.

IV. FOUR PHOTON EVENTS

We now turn to new processes mediated by unparticle self-interactions. As noted in Sec. I, the 3-point function is particularly interesting, and, depending on the unparticle interactions with the standard model, may mediate a variety of processes leading to spectacular 4-body final states.

As an example, in this section we consider the four photon signal shown in Fig. 1.

The cross sections for $gg, q\bar{q} \rightarrow \mathcal{U} \rightarrow \mathcal{U}\mathcal{U} \rightarrow \gamma\gamma\gamma\gamma$ are completely specified, given the Feynman rules of Eqs. (3) and (6). With momenta as labeled in Fig. 1, we find

$$\begin{aligned} |\overline{\mathcal{M}}_{gg \rightarrow 4\gamma}|^2 &= 2^{10} \left| \frac{c_g c_\gamma^2}{\Lambda_4^{3d}} \right|^2 (p_a \cdot p_b)^2 (p_1 \cdot p_2)^2 \\ &\quad \times (p_3 \cdot p_4)^2 |\langle 0 | O(q_2) O(q_3) O^\dagger(q_1) | 0 \rangle|^2 \end{aligned} \quad (11)$$

$$\begin{aligned} |\overline{\mathcal{M}}_{q\bar{q} \rightarrow 4\gamma}|^2 &= \frac{2^9}{3} \left| \frac{e c_4^f c_\gamma^2}{\Lambda_4^{3d}} \right|^2 v^2 (p_a \cdot p_b) (p_1 \cdot p_2)^2 \\ &\quad \times (p_3 \cdot p_4)^2 |\langle 0 | O(q_2) O(q_3) O^\dagger(q_1) | 0 \rangle|^2, \end{aligned} \quad (12)$$

where we have averaged and summed over initial and final state colors and polarizations, but have not yet included the factor $1/4!$ to account for the four identical photons in the final state. To evaluate the parton-level cross sections, we use the results of Sec. II for the 3-point correlation function. Setting $c_g = c_\gamma = 1$ and $e^2(c_4^f)^2 = 2\pi$ as above, and integrating over 4-body phase space with the Monte Carlo program VEGAS [20], we find that the parton-level cross sections may be written as

$$\hat{\sigma}_{gg \rightarrow 4\gamma}(\hat{s}) = f_d^g C_d^2 \left(\frac{\hat{s}}{\Lambda_4^2} \right)^{3d} \frac{1}{(\hat{s}/[\text{GeV}^2])} [\text{fb}] \quad (13)$$

$$\hat{\sigma}_{q\bar{q} \rightarrow 4\gamma}(\hat{s}) = f_d^q C_d^2 \left(\frac{\hat{s}}{\Lambda_4^2} \right)^{3d} \left(\frac{v^2}{\hat{s}} \right) \frac{1}{(\hat{s}/[\text{GeV}^2])} [\text{fb}], \quad (14)$$

where the dimensionless proportionality factors f_d^g and f_d^q are given in Table I.

TABLE I. Dimensionless parton-level proportionality factors $f_d^{g,q}$, and unparticle 4γ reference cross sections at the Tevatron ($\sqrt{s} = 1.96 \text{ TeV}$), LHC ($\sqrt{s} = 14 \text{ TeV}$) and ILC ($\sqrt{s} = 1 \text{ TeV}$). These reference cross sections assume $\Lambda_4 = 1 \text{ TeV}$ and $C_d = 1$; the actual cross sections scale with C_d^2/Λ_4^{6d} . Upper bounds on this combination of parameters from existing data at the Tevatron are also listed, as are the resulting maximum cross sections possible at the LHC and ILC.

	d = 1.1	d = 1.2	d = 1.5	d = 1.9
f_d^g	2.7	1.2	0.16	0.02
f_d^q	5.5	2.5	0.35	0.04
Tevatron $\sigma_{q\bar{q} \rightarrow 4\gamma}^{\text{ref}}$ [fb]	2×10^{-8}	6×10^{-9}	2.5×10^{-10}	1.5×10^{-11}
Tevatron $\sigma_{gg \rightarrow 4\gamma}^{\text{ref}}$ [fb]	3×10^{-9}	7×10^{-10}	2×10^{-11}	6×10^{-13}
Tevatron upper bounds on $C_d/(\Lambda_4[\text{TeV}])^{3d}$	1.3×10^4	2.3×10^4	1.2×10^5	4.8×10^5
LHC $\sigma_{gg \rightarrow 4\gamma}^{\text{ref}}$ [fb]	2.6×10^{-5}	1.7×10^{-5}	1.3×10^{-5}	3.5×10^{-5}
LHC $\sigma_{q\bar{q} \rightarrow 4\gamma}^{\text{ref}}$ [fb]	1.0×10^{-6}	6×10^{-7}	3.6×10^{-7}	1.0×10^{-6}
LHC maximum cross section [fb]	4300	9600	1.8×10^5	8.4×10^6
ILC $\sigma_{e^+e^- \rightarrow 4\gamma}^{\text{ref}}$ [fb]	1.0×10^{-6}	4.7×10^{-7}	6.0×10^{-8}	8.0×10^{-9}
ILC maximum cross section [fb]	160	250	810	1900

A. Bounds from Tevatron

The 4γ unparticle signal is bounded by searches at the Tevatron. The D0 collaboration has searched for the inclusive production of multiphoton final states [23]. Events are selected with three or more photons in the central calorimeter ($|\eta| < 1.1$) and E_T -ordered cuts on their transverse energies: $E_T^{1,2,3(4)} > 30, 20, 15(15)$ GeV. The dominant backgrounds are diphoton production with additional initial state radiation photons and events in which jets or electrons are misidentified as photons. No excess of events above the standard model prediction was found in the Tevatron data with integrated luminosity $0.83 \pm 0.05 \text{ fb}^{-1}$ collected during 2002–2005.

This search result thus sets upper bounds on combinations of the unparticle self-interaction strength C_d and the energy scale Λ_4 . To derive these bounds, we again set $c_g = c_\gamma = 1$ and $e^2(c_d^f)^2 = 2\pi$. As with the $\gamma\gamma$ signal discussed in Sec. III, at the Tevatron, the $q\bar{q}$ contribution dominates over that from gg , since $p\bar{p}$ collisions provide a large density of antiquarks, and at $\sqrt{s} = 1.96$ TeV, large Bjorken x is required.

We impose the kinematic cuts on rapidities and transverse energy as given above. Estimating the background event rate to be $\mathcal{L}\sigma_{q\bar{q}\rightarrow 4\gamma}^{\text{SM}} \approx \mathcal{L}(\sum_q Q_q^2)(\alpha/\pi)^2 \sigma_{q\bar{q}\rightarrow 2\gamma}^{\text{SM}} \sim 0.83 \text{ fb}^{-1} \times (0.002)^2 \times 0.66 \text{ pb} \sim \mathcal{O}(10^{-3})$, we find that it is negligible. The 95% CL upper limit of 3.04 events for zero background and zero events observed therefore becomes the 95% CL bound

$$C_d^2 \left(\frac{1}{\Lambda_4 [\text{TeV}]} \right)^{6d} \leq \frac{3.04}{0.83 \text{ fb}^{-1} \sigma_{\text{tot}}^{\text{ref}}}, \quad (15)$$

where $\sigma_{\text{tot}}^{\text{ref}} \equiv \sigma_{q\bar{q}\rightarrow 4\gamma}^{\text{ref}} + \sigma_{gg\rightarrow 4\gamma}^{\text{ref}}$ is the total reference cross section, determined by setting $\Lambda_4 = 1$ TeV and $C_d = 1$. The resulting upper bounds on C_d/Λ_4^{3d} are given in Table I.

B. Prospects for LHC and international linear collider

We now determine the LHC cross sections for 4γ production mediated by unparticle self-interactions. Using VEGAS [20], we Monte Carlo simulate 4 to 10×10^6 events for several values of d . We require the photons to have rapidity $|\eta| < 2.5$ and transverse energies $E_T^{1,2,3,4} > 30, 20, 15, 15$ GeV. The resulting reference cross sections for $\Lambda_4 = 1$ TeV and $C_d = 1$ from gg and $q\bar{q}$ initial states are given in Table I.

Of course, the actual cross sections scale with C_d^2 . We do not know of any way to bound C_d theoretically, or, indeed, to specify a “typical” value for C_d . Lacking theoretical guidance, we simply impose existing experimental bounds. Although bounds on unparticles have been discussed at length in the literature, these constraints, including those derived and presented in Sec. III, do not bound C_d . For a direct bound, we must therefore turn to the Tevatron results derived above, which, of course, constrain C_d and Λ_4 in the

combination identical to that which enters the LHC cross section. Assuming these parameters saturate the bound of Eq. (15), we find the maximal cross sections presented in Table I and plotted in Fig. 4. These cross sections are extraordinarily large, ranging from picobarns for $d = 1.1$ to nanobarns for $d = 1.9$. If the unparticle self-interaction is anywhere near the largest values allowed by current experimental constraints, this spectacular signal will be discovered very early at the LHC.

The p_T distributions of the leading, next-to-leading, next-next-to-leading, and fourth photons in unparticle 4γ events are given in Fig. 5. We find that the p_T spectra, even for the third and fourth photon, are remarkably hard. Given this, the standard model background of diphoton production with two initial state radiation photons can be eliminated with p_T cuts with little effect on the signal. The dominant backgrounds will be from events with misidentified jets or electrons, but even these may be reduced significantly with hard p_T cuts without large reduction in the signal. It would be very interesting to determine the extent to which this is validated by a realistic detector study. Last, we note that the shapes of the p_T distributions, along with other kinematic information, are, of course, independent of C_d and Λ_4 . They may therefore be used to identify unparticles as the source of these signals, and to distinguish them from anomalies predicted by other frameworks for new physics.

If the coupling of scalar unparticles to electrons is of the same size as to quarks, 4γ event rates at the international linear collider (ILC) can be calculated with Eq. (14) multiplied by 3. ILC reference cross sections and maximal possible cross sections are presented in Table I and Fig. 4. Interestingly, the 4γ cross section at a 1 TeV ILC is about 2 orders of magnitude larger than at the Tevatron. This is because the parton densities become less than one

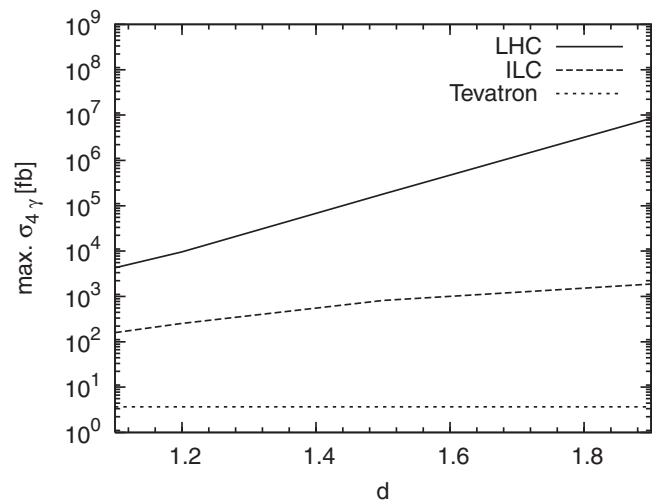


FIG. 4. Maximum possible cross sections for 4γ production through unparticle self-interactions, given existing bounds on 4γ events from the D0 Collaboration at the Tevatron [23].

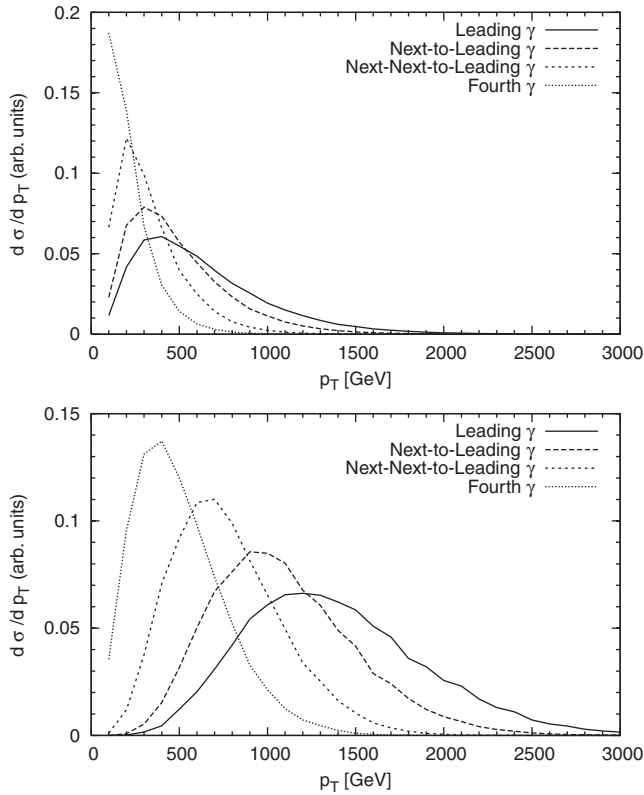


FIG. 5. The p_T distributions for p_T -ordered photons in unparticle 4γ events (from the dominant gg initial state only) at the LHC for $d = 1.1$ (top) and 1.9 (bottom).

for $x \geq 0.3$, so the Tevatron $p\bar{p} \rightarrow 4\gamma$ cross section is dominated by the contribution from $\sqrt{\hat{s}} \sim 300$ GeV.

V. DISCUSSION

In this work, we have investigated a new feature of unparticle physics, namely, the self-interactions of unparticles. Such interactions are necessarily present in conformal theories, are unsuppressed for strongly-coupled conformal sectors, and introduce a large range of new phenomena not studied previously.

As an example, we have investigated the 3-point correlation function in detail. This is completely specified by

conformal invariance,¹ up to a constant C_d , and mediates a host of processes, such as $pp \rightarrow \mathcal{U} \rightarrow \mathcal{U}\mathcal{U} \rightarrow \gamma\gamma\gamma\gamma, \gamma\gamma ZZ, ZZZZ, \gamma\gamma l^+ l^-, ZZ l^+ l^-, 4l$ at the LHC. We know of no upper bound on C_d . We have therefore imposed only the existing Tevatron bounds, and have found that, for the example 4γ signal discussed here, the allowed cross sections at the LHC are enormous, ranging from picobarns for unparticle dimension $d = 1.1$ to nanobarns for $d = 1.9$. Such signals could emerge very early after the LHC turns on, and imply that the 4-body final states could be by far the most promising modes for unparticle discovery at colliders. Given these observations, it would be very interesting to perform similar analyses for the other final states, as well as to carry out realistic detector simulations to determine the extent to which jet and lepton misidentification masks these *a priori* spectacular signals.

On the theoretical side, the most pressing issue is to determine what values of C_d are possible or natural. Conformal invariance by itself does not determine the constant, and we are unaware of any other consistency conditions that could bound C_d . It would be very interesting to see if the AdS/CFT correspondence can shed light on this issue. In the absence of theoretical bounds, C_d can be large, and $pp \rightarrow \mathcal{U}\mathcal{U} \rightarrow 4\gamma$ and related 4-body final states may have cross sections larger than $pp \rightarrow \mathcal{U} \rightarrow \gamma\gamma$ and related 2-body states. Such a conclusion is highly counter intuitive, but perhaps possible, given the other surprising properties of unparticles discovered so far.

ACKNOWLEDGMENTS

We thank Yuri Shirman and Matt Strassler for interesting discussions. The work of J.L.F. is supported in part by NSF Grants No. PHY-0239817 and No. PHY-0653656, NASA Grant No. NNG05GG44G, and the Alfred P. Sloan Foundation. The work of A.R. is supported in part by NSF Grants No. PHY-0354993 and No. PHY-0653656. The work of H.T. is supported in part by NASA Grant No. NNG05GG44G.

¹The importance of self-interactions in the case of broken conformal symmetry has also been recently emphasized in Ref. [14].

- [1] H. Georgi, Phys. Rev. Lett. **98**, 221601 (2007).
- [2] See, e.g., T. Banks and A. Zaks, Nucl. Phys. **B196**, 189 (1982).
- [3] See, e.g., K. A. Intriligator and N. Seiberg, Nucl. Phys. B, Proc. Suppl. **45B, C**, 1 (1996).
- [4] H. Georgi, Phys. Lett. **650B**, 275 (2007).
- [5] K. Cheung, W. Y. Keung, and T. C. Yuan, Phys. Rev. Lett. **99**, 051803 (2007).

- [6] M. A. Stephanov, Phys. Rev. D **76**, 035008 (2007).
- [7] P. J. Fox, A. Rajaraman, and Y. Shirman, Phys. Rev. D **76**, 075004 (2007).
- [8] A. Delgado, J. R. Espinosa, and M. Quiros, J. High Energy Phys. **10** (2007) 094.
- [9] M. Bander, J. L. Feng, A. Rajaraman, and Y. Shirman, Phys. Rev. D **76**, 115002 (2007).
- [10] N. Greiner, Phys. Lett. **653B**, 75 (2007).

- [11] M. C. Kumar, P. Mathews, V. Ravindran, and A. Tripathi, arXiv:0709.2478.
- [12] S. L. Chen and X. G. He, Phys. Rev. D **76**, 091702 (2007); P. Mathews and V. Ravindran, Phys. Lett. **657B**, 198 (2007); T. G. Rizzo, J. High Energy Phys. **10** (2007) 044; K. Cheung, W. Y. Keung, and T. C. Yuan, Phys. Rev. D **76**, 055003 (2007); S. L. Chen, X. G. He, and H. C. Tsai, J. High Energy Phys. **11** (2007) 010; T. Kikuchi and N. Okada, arXiv:0707.0893; D. Choudhury and D. K. Ghosh, arXiv:0707.2074; H. Zhang, C. S. Li, and Z. Li, Phys. Rev. D **76**, 116003 (2007); Y. Nakayama, Phys. Rev. D **76**, 105009 (2007); N. G. Deshpande, X. G. He, and J. Jiang, Phys. Lett. **656B**, 91 (2007); G. Cacciapaglia, G. Marandella, and J. Terning, J. High Energy Phys. **01** (2008) 070; M. Neubert, Phys. Lett. **660**, 592B (2008); M. x. Luo, W. Wu, and G. h. Zhu, Phys. Lett. **659B**, 349 (2008); Y. Liao, arXiv:0708.3327; A. T. Alan and N. K. Pak, arXiv:0708.3802; T. i. Hur, P. Ko, and X. H. Wu, Phys. Rev. D **76**, 096008 (2007); S. Majhi, arXiv:0709.1960; A. T. Alan, N. K. Pak, and A. Senol, arXiv:0710.4239; O. Cakir and K. O. Ozansoy, arXiv:0710.5773; I. Sahin and B. Sahin, arXiv:0711.1665; A. T. Alan, arXiv:0711.3272; K. Huitu and S. K. Rai, Phys. Rev. D **77**, 035015 (2008); J. R. Mureika, Phys. Lett. **660B**, 561 (2008); O. Cakir and K. O. Ozansoy, arXiv:0712.3814; T. Kikuchi, N. Okada, and M. Takeuchi, arXiv:0801.0018.
- [13] M. J. Strassler and K. M. Zurek, Phys. Lett. **651B**, 374 (2007); arXiv:hep-ph/0605193; T. Han, Z. Si, K. M. Zurek, and M. J. Strassler, arXiv:0712.2041.
- [14] M. J. Strassler, arXiv:0801.0629.
- [15] G. Mack, Commun. Math. Phys. **55**, 1 (1977).
- [16] B. Grinstein, K. Intriligator, and I. Z. Rothstein, arXiv:0801.1140.
- [17] Y. Nakayama, Phys. Rev. D **76**, 105009 (2007).
- [18] T. Aaltonen *et al.* (CDF Collaboration), Phys. Rev. Lett. **99**, 171801 (2007).
- [19] H. L. Lai *et al.* (CTEQ Collaboration), Eur. Phys. J. C **12**, 375 (2000).
- [20] G. P. Lepage, J. Comput. Phys. **27**, 192 (1978).
- [21] G. J. Feldman and R. D. Cousins, Phys. Rev. D **57**, 3873 (1998).
- [22] T. Sjostrand, S. Mrenna, and P. Skands, J. High Energy Phys. **05** (2006) 026.
- [23] D0 Collaboration, D0 Note 5067-CONF.